Modelling of the Effects of Friction and Compression on Explosives

Problem presented by

John Curtis

Atomic Weapons Establishment

Executive Summary

The Atomic Weapons Establishment (AWE) investigate the safe use and handling of high explosives. High explosives are inherently dangerous and their detonation can be triggered by low velocity impacts with speeds in the range of 10 to 70 m s^{-1}. The kinetic energy associated with impact is converted into thermal energy within the explosive, potentially leading to thermal runaway and detonation.

The study group was asked to investigate the mechanisms generating heat and detonation in an explosive HMX, based on the compression of a sample of the explosive. The study group identified frictional heating in localized shear bands as the most likely mechanism for heat generation in the compression of both HMX and other high explosives formed from a granular material within a polymer bonding. The study group also considered the squeezing of explosive samples for a range of more general rheologies and investigated possible improvements to the numerical modelling already conducted by AWE.

Version 1.0
June 12, 2011
iii+17 pages

Report authors

Peter Hicks (University of East Anglia)
Cameron Hall (Oxford University)

Contributors

Victoria Andrew (Manchester University)
David Binding (Aberystwyth University)
Matthew Crooks (Manchester University)
John Curtis (Atomic Weapons Establishment)
Mohit Dalwadi (Oxford University)
Russell Davies (Cardiff University)
Michelle De Decker (Centre de Recerca Matemàtica)
Francesc Font (Centre de Recerca Matemàtica)
Małgorzata Frąszczak (CIAMSE & Poznan University)
Cameron Hall (Oxford University)
Peter Hicks (University of East Anglia)
Ikenna Ireka (Obafemi Awolowo University)
Andrew Lacey (Heriot-Watt University)
Cara Morgan (Oxford University)
Ellen Murphy (Limerick University)
John Ockendon (Oxford University)
Richard Purvis (University of East Anglia)
Melanie Roberts (University of Western Australia)
Tom Shearer (Manchester University)
Emma Warneford (Oxford University)
Zhiyan Wei (Harvard University)

Contents

1 Introduction

1.1 Background and scope

(1.1.1)   The study group was asked to investigate the behaviour of explosives when subjected to an impact by a solid body at speeds between 10 and 70 m s^{-1}. Such an impact is described as an insult in the literature concerned with the study of high explosives. The energy associated with an insult can be converted into heat within the explosive, which can produce thermal runaway and ultimately lead to detonation.

(1.1.2)   The Atomic Weapons Establishment (AWE) are interested in determining conditions for the safe handling of high explosives in order to prevent accidents. AWE would like to understand the response of a sample of high explosive to an insult at a range of impact speeds, in order to determine the response of a sample to being accidentally hit or dropped and thereby to minimize the risk of accidental detonation.

(1.1.3)   The current test used by AWE to determine the response of explosive samples to impact is the UK Steven test (see Figure 1). This test consists of fixing a small sample of explosive material between a base unit and a covering plate, while surrounding it with a strong retaining ring. The cover plate is then hit by a curved projectile in order to examine the response of the explosive to the insult. As the impact speed is increased more energy is transferred to the explosive, thereby increasing the risk of detonation.
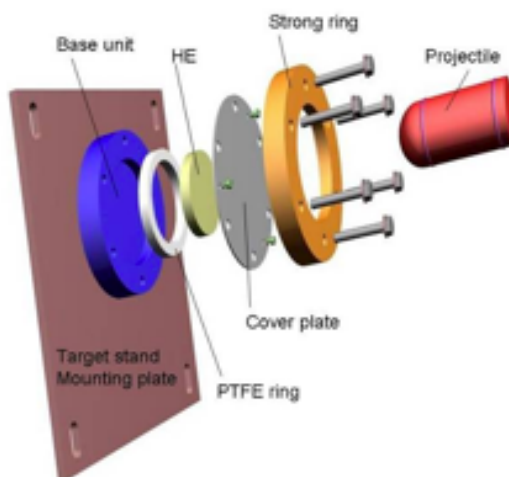

Figure 1: The UK Steven Test apparatus [4]

(1.1.4)   The study group was asked to investigate the following problems:
- Can we analytically model the response of the explosive in the Steven Test and/or similar tests in simpler geometrical configurations?

- What are the appropriate rheologies for the modelling of high explosives? Are elastic or plastic models more appropriate?

- What is the primary mechanism for heat generation in a sample of high explosive undergoing compression? Is heat generated by friction with either the walls or with internal impurities (e.g. grit) in the sample?

- If heat is generated by friction or some other mechanism, where does the heat go and how could it lead to explosive ignition?

1.2 Material Properties: The behaviour of HMX

(1.2.1)   It is difficult to obtain detailed information about the rheological properties of HMX because of the danger involved in performing experiments on high explosives.

(1.2.2)   One class of experiments used to gain information about the material properties of HMX are unconfined compression tests. Although generally performed at lower strain rates than the Steven test, these give useful information about the stress-strain curve in the simple configuration of pure compression [12].
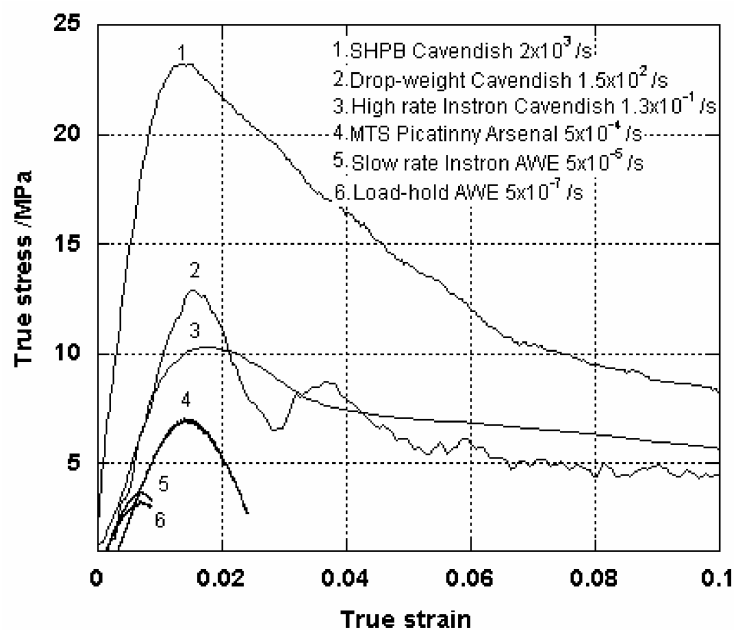

Figure 2: Stress-strain curves for a range of different strain rates, taken from Williamson *et al.* [12].

(1.2.3)   Typical stress-strain curves at a variety of different strain rates are shown in Figure 2, taken from [12]. In each case, efforts were made to keep

2

the strain rate constant, and thus measure the stress corresponding to a linearly increasing strain.

(1.2.4)   Interestingly, the elastic modulus appears to be larger at higher strain rates, and the strain corresponding to maximum stress only increased minimally with increasing strain rate. It was agreed that the best apparent model for the stage before yield is an elastic solid with a strain-rate dependent elastic modulus.

(1.2.5)   The yielding behaviour is very interesting because of the significant decrease in stress shown in Figure 2. Such strain softening is indicative of possible shear banding, where the flow localises to narrow bands within the solid. Since this localised flow might lead to hotspots, shear banding was identified as an important phenomenon for further investigation.

2   Shear banding

2.1   Introduction to shear bands

(2.1.1)   Shear banding is a strain-localisation phenomenon in which an applied stress is relieved by plastic flow in narrow planar regions (the shear bands). This is in contrast to classical plasticity, where flow is assumed to be uniform throughout any region in which the yield stress has been reached.

(2.1.2)   Shear banding is an especially important mode of failure in granular materials, in polymers, and in ductile materials. Since HMX is a granular material held together with a polymer bonding agent, it might be expected that shear banding plays a role in HMX plasticity.

(2.1.3)   Because the plastic flow is localised when shear bands occur, it follows that there is also localised energy release. In the context of high explosives, this means that shear bands might be associated with hot-spots and other regions of localised heating that can lead to ignition.

(2.1.4)   Indeed, the fundamental mechanism of shear banding in metals and polymers is thought to be strain-softening due to thermal effects. As plastic flow occurs through a material, the heating due to dissipation of mechanical energy causes the material to soften and become easier to strain. This then leads to instabilities, so that small fluctuations in the flow accelerate, causing all of the strain to localise into small bands. If additional energy were available from an exothermic reaction in the heated regions, this would further exacerbate the thermal softening and concomitant strain localisation.

2.2 Experimental evidence of shear banding in high explosives

(2.2.1)   Williamson *et al.* [12] performed quasistatic compression tests on EDC37, a polymer-bonded explosive, in which they observed clear evidence of the formation of shear bands at all temperatures, all shear rates, and all aspect ratios. Photographs of shear banding from [12] are shown in Figure 3.
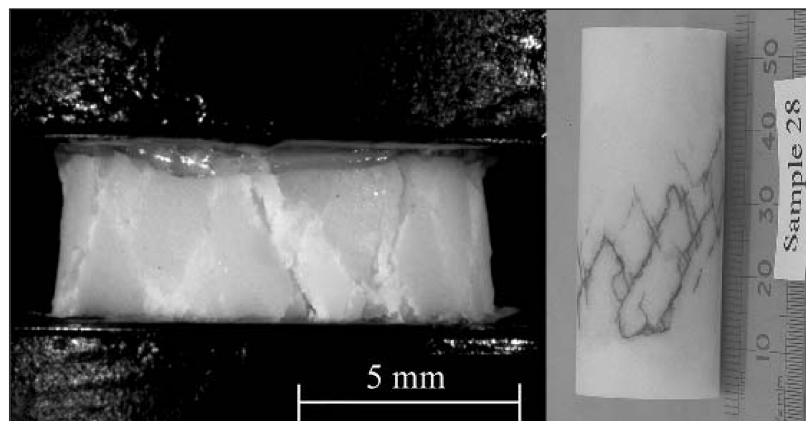

Figure 3: Photograph of shear bands in EDC37 [12].

(2.2.2)   Similarly, Balzer *et al.* [1] performed drop-weight tests on other high explosives (PETN and RDX) where results were recorded using heat-sensitive film. They observed stripes of localised heating that they identified with shear bands acting as planar heat sources.

(2.2.3)   Additionally, the stress-strain curve observed in Figure 2 is characteristic of the strain-softening observed in adiabatic shear banding [13].

(2.2.4)   Another intriguing piece of experimental work by Clancy *et al.* [3] discusses damage localisation in a high explosive (PBX-9501) in the context of brittle crack formation. It is possible, however, that they too were observing shear banding.

(2.2.5)   From this experimental evidence, it seems likely that shear banding, and possibly other forms of damage localisation, are significant in the mechanical failure of high explosives. Indeed, the combined observations that shear banding is observed at comparatively mild strain-rates [12] and that shear banding leads to observable local heating [1] suggests that shear banding will be important in the Steven test and other related experiments, and may be a key factor in ignition.
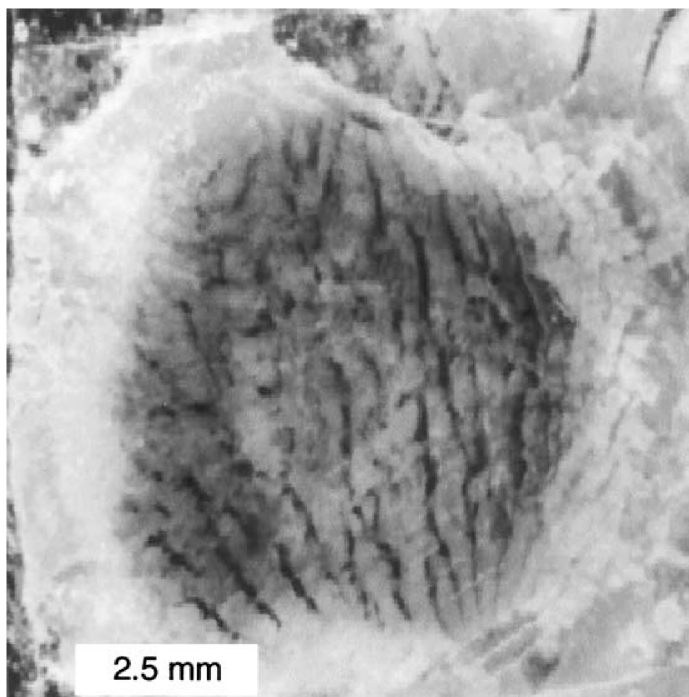
4

Figure 4: Photograph of heating due to shear bands in PETN or RDX [1].

2.3 Theoretical models of shear banding

(2.3.1) In a literature search, no mathematical models specific to shear banding in high explosives (or, more generally, polymer-bonded granular materials) were found.

(2.3.2) The most elementary models of shear banding in metals [15, 14] involve coupling a plastic constitutive law with thermal softening to an equation for heat flow. This leads to interesting instabilities that can be interpreted as indicating shear banding.

(2.3.3) The simplest configuration for modelling shear banding (and the one explored most often in these models) is a slab under simple shear, as in Figure 5. In such a situation, we expect shear bands to run parallel with the sliding plates, and the spacing between bands to be governed by the interplay between dissipative heating and thermal conduction.

(2.3.4) A simplistic but instructive approach to shear banding (based on more detailed work by Andrew Lacey [2]) is to consider the situation of a thermo-viscous material with a power-law relationship between stress and velocity
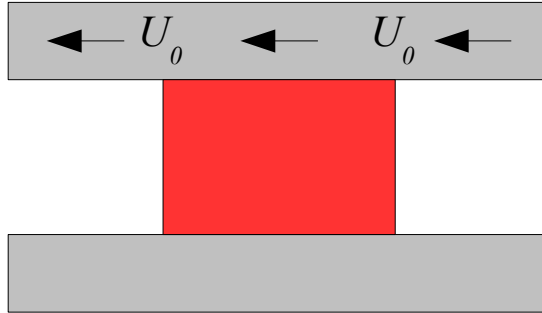
Figure 5: A sample of explosive (or inert explosive substitute) subject to pure shear.

gradient. In the simple shear configuration of 5, this leads to

$$\frac{\partial \tau}{\partial x} = 0, \tag{1a}$$

$$\frac{\partial \theta}{\partial t} = \varepsilon \frac{\partial^2 \theta}{\partial x^2} + \tau \frac{\partial v}{\partial x}, \tag{1b}$$

$$\frac{\partial v}{\partial x} = f(\theta)\tau^k, \tag{1c}$$

where τ represents stress, θ represents temperature, ε is the thermal conductivity, v represents velocity, $f(\theta)$ represents the temperature-dependent viscous compliance, x represents distance across the sheared material, and t represents time.

(2.3.5) In the limit of low thermal conductivity ($\varepsilon \to 0$), and with initial conditions where there is a small temperature disturbance, it is possible to obtain explicit solutions for some choices of $f(\theta)$. One such choice is $f(\theta) = \exp(\theta)$, subject to initial conditions

$$\theta(x,0) = \begin{cases} 0 & \alpha < |x| < 1, \\ \beta & |x| < \alpha, \end{cases} \tag{2}$$

(2.3.6) Under a constant applied stress, $\bar{\tau}$, we then recover

$$\theta_1 = -\log(e^{-\beta} - \bar{\tau}t), \tag{3a}$$

$$\theta_2 = -\log(1 - \bar{\tau}t), \tag{3b}$$

where θ_1 is the temperature in the region $|x| < \alpha$, and θ_2 is the temperature where $\alpha < |x| < 1$.

(2.3.7) Even without additional heating from an exothermic reaction, we find that the difference in temperature between the two regions increases over time and that the strain becomes localised into the warmer region.

(2.3.8) More realistic models of this phenomenon are needed, as are methods for exploring shear banding and other forms of strain localisation in the context of the complex deformation of a larger body.

(2.3.9) Additionally, it would be useful to perform simple shear experiments on high explosives or other similar bonded granular materials. This could yield valuable data on the exact nature of shear banding in high explosives, and the results would be much easier to compare with model results than data from the Steven test.

3 Squeeze flow behaviour with alternative rheologies

3.1 Material behaviour in squeezing flows

(3.1.1) AWE conduct tests on a wide range of explosives with differing material properties. Many of these materials potentially behave differently to HMX under compression. AWE have also worked on numerical simulations of the Steven test. Simple analytical solutions of materials under compression are therefore of interest.

(3.1.2) A test not currently conducted by AWE, but which is of interest, is the "Pinch" test, where a sample of explosive is squeezed between two parallel plates without the confining rings seen in the Steven test. It is envisaged in the AWE "Pinch" test that the upper top plate is moved towards a stationary lower plate. In Figure 6 a similar squeezing flow is shown in which both plates move towards each other. These two situations are equivalent up to a change in the frame of reference. A review of squeeze flows for the geometry shown in Figure 6 and for a range of different rheologies has been conducted by Engmann *et al.* [5]. The most relevant of rheologies for the evolution of explosive samples are discussed in the next sections.

3.2 Perfectly plastic with free slip boundary conditions

(3.2.1) If plastic waves are assumed to travel through the sample very rapidly, then the material subsequently acts as a perfect plastic. In two dimensions (x, y), for small deformations of the explosive, the velocity profile is given by

$$u = -\frac{h'(t)\,x}{h(t)}, \qquad\qquad v = \frac{h'(t)\,y}{h(t)}, \qquad (4)$$

where $h'(t) = -U_0$. Consequently the velocity profiles correspond to plug flow.
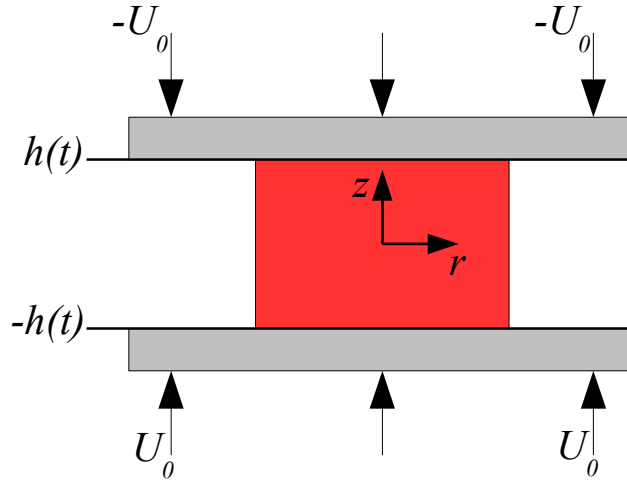
Figure 6: A sample of explosive (or inert explosive substitute) squeezed between two parallel plates.

(3.2.2)   In this case the dissipation

$$\sigma_{ij}\epsilon_{ij} = \frac{2U_0 Y}{\sqrt{3}\left[h_0 - U_0\left(t - t_0\right)\right]} \tag{5}$$

is constant through the flow, which is not consistent with the existing numerical computations. Here Y is the yield stress of the sample. In this model perfect slip is assumed at the edge of the explosive, where as in reality the presence of the solid body will impede the motion of the explosive, leading to more complicated velocity profiles and increased dissipation close to the solid boundaries.

3.3   Perfectly plastic with frictional slip boundary conditions

(3.3.1)   A similar problem in axisymmetry has been studied with frictional slip at the boundaries [10]. Here, the stress on the boundary is given by $\sigma_{xy} = mY$, where Y is the yield stress of the explosive and the coefficient m varies between 0 (for free slip), and 1 (when the stress at the boundary equals the yield stress). In this case the radial and vertical velocity components are given by

$$u_r = \frac{U_0 r}{h} + \frac{\sqrt{3}U_0}{m}\left(1 - \frac{4m^2 z^2}{h^2}\right)^{1/2} - Ch, \tag{6a}$$

$$u_z = -\frac{2U_0 z}{h} - \frac{\sqrt{3}U_0 h}{4mr}\left[\frac{\arcsin(2mz/h)}{m} + \frac{2z}{h}\sqrt{1 - \frac{4m^2 z^2}{h^2}}\right] + Cz, \tag{6b}$$

where

$$C = \frac{\sqrt{3}U_0}{4m}\left[\left(1 - m^2\right)^{1/2} + \frac{\arcsin(m)}{m}\right], \tag{7}$$

8

and z and r are the vertical and radial directions respectively and U_0 is the velocity of the plates.
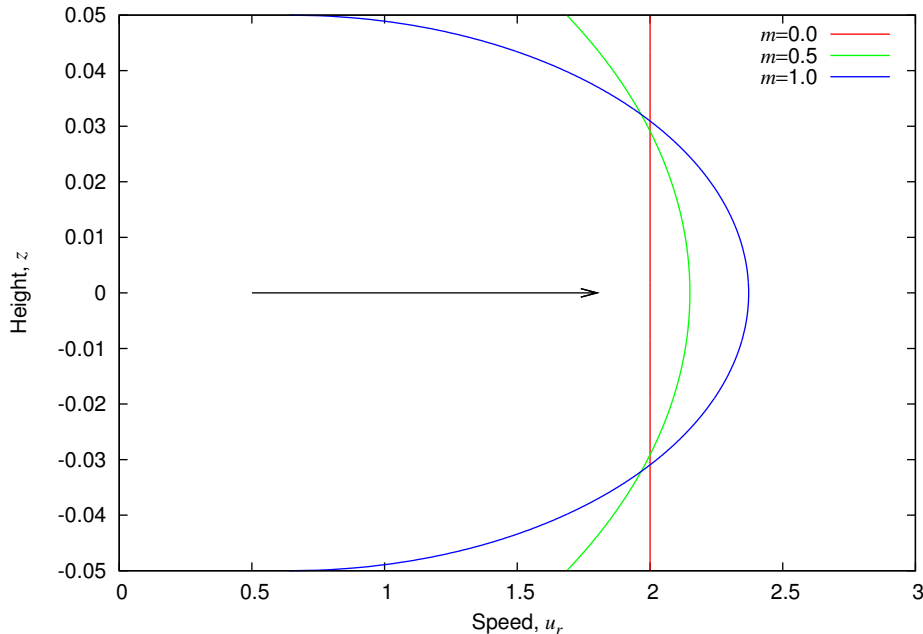

Figure 7: Velocity profiles for a range of slip coefficients at a radius $r = 0.2$ and a squeezing velocity $U_0 = 1$.

(3.3.2)   Radial velocity profiles as functions of gap height are shown for $m = 0.0$ (plug flow), 0.5 and 1.0, at a radius $r = 0.2$ from the centre. For $m > 0$, the frictional slip at the boundary acts to reduce the velocity in this region. Note unlike a viscous fluid, once the yield stress is achieved in a perfectly plastic material, some slip at the boundaries is inevitable and this is seen in all cases. However, for $m > 0$ the dissipation of energy will be greatest close to the boundaries. This is consistent with the temperature rise seen in the numerics.

3.4   Viscous fluid

(3.4.1)   In a pinch experiment where the vertical separation of the plates is much smaller than their horizontal extent, the flow of a viscous fluid is considered as a highly idealized model of an explosive sample subject to the pinch test. In this case a lubrication model is appropriate and fluid inertia can be neglected. In the geometry shown in Figure 6, the radial component of the fluid velocity is given by

$$u_r = -\frac{3U_0 r^2}{h^3} \left(z - h \right) \left(z + h \right). \tag{8}$$

9

In this small aspect ratio the leading order contribution to the dissipation is given by

$$\Phi \sim \mu \left(\frac{\partial u}{\partial z}\right)^2 = \frac{36\mu U_0^2 r^4 z^2}{h^6}, \tag{9}$$

where μ is the fluid viscosity. Consequently, energy dissipation generates the most heat at the boundaries of the squeeze film. The horizontal velocity component and the dissipation are shown in Figure 8 as functions of the height across the gap at a radius $r = 0.2$ for $U_0 = 1$ and $h(t) = 0.05$.
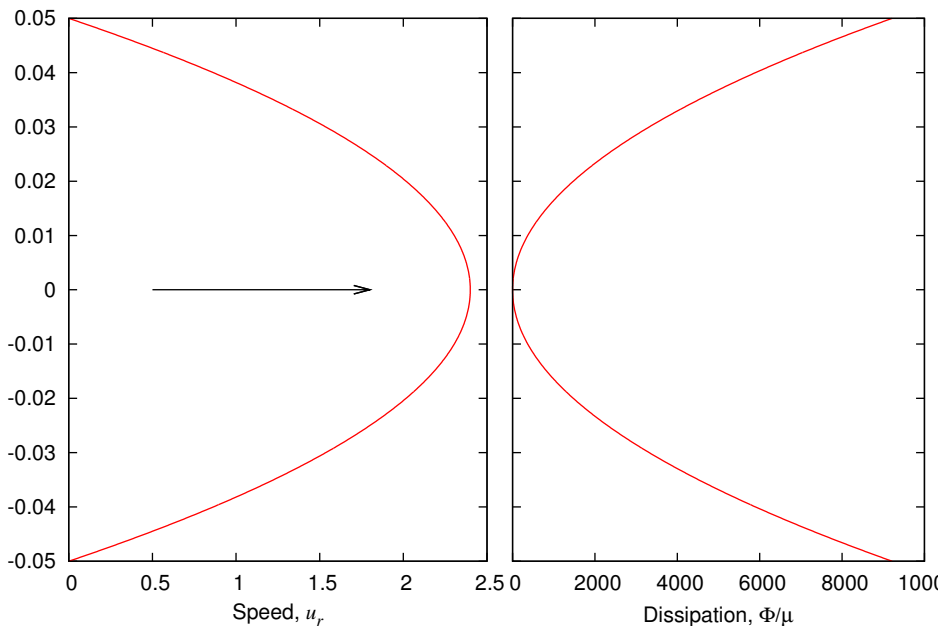
Figure 8: Velocity profiles (left) and the viscous dissipation (right) for a viscous fluid in a squeeze film at a radius of $r = 0.2$ from the centre and with the squeezing velocity $U_0 = 1$.

(3.4.2)   This idealised model mimics the behaviour seen in the numerical simulations conducted by AWE, with the greatest heating occurring close to the sample boundaries. However, in this small aspect ratio flow the term in the energy conservation equation corresponding to dissipation is much smaller than the term corresponding to the vertical diffusion of temperature through the sample [7]. Therefore, in a small aspect ratio viscous fluid squeeze film the temperature profiles are independent of height.

(3.4.3)   More general solutions of the Navier-Stokes equations including inertia and larger plate separations are available for some proscribed plate separations and also a constant force on each plate [11].

3.5 Viscoelastic solid

(3.5.1)   An incompressible, viscoelastic fluid with velocity $\mathbf{u}$, density ρ and pressure p is considered with the same geometry as Figure 6, but varying from $z = 0$ to $h(t)$. The conservation of mass implies

$$\nabla \cdot \mathbf{u} = 0, \tag{10}$$

while conservation of momentum is given by

$$\rho \left(\mathbf{u}_t + (\mathbf{u} \cdot \nabla) \mathbf{u} \right) = -\nabla p + \nabla \cdot \boldsymbol{\tau}', \tag{11}$$

where $\boldsymbol{\tau}'$ is the stress tensor.

(3.5.2)   For the fluid we are considering, a Maxwell Oldroyd-B model for the stress tensor $\boldsymbol{\tau}'$ is used, which is given by

$$t_r \overset{\triangle}{\boldsymbol{\tau}'} + \boldsymbol{\tau}' = 2\eta D, \tag{12}$$

where t_r is the relaxation time, η is the material viscosity, D is the deformation rate tensor and $\overset{\triangle}{\boldsymbol{\tau}'}$ is the upper convected time derivative of the stress tensor. $\overset{\triangle}{\boldsymbol{\tau}'}$ is given by

$$\overset{\triangle}{\boldsymbol{\tau}'} = \frac{\partial \boldsymbol{\tau}'}{\partial t} + \mathbf{u} \cdot \nabla \boldsymbol{\tau}' - (\nabla \boldsymbol{u})^T \cdot \boldsymbol{\tau}' - \boldsymbol{\tau}' \cdot (\nabla \boldsymbol{u}). \tag{13}$$

(3.5.3)   Following work done by Engmann *et al.* [5] for a 2-D flow we can write the velocities u, v in the r and z directions as

$$u = -\frac{r\dot{h}}{2h} g'(\nu, \tau), \quad \text{and} \quad v = \dot{h} g(\nu, \tau), \tag{14}$$

respectively. The boundary conditions are

$$u = v = 0 \quad \text{on} \quad \nu = 0, \quad \text{and} \quad u = 0, \ v = \dot{h} \quad \text{on} \quad \nu = 1, \tag{15}$$

where

$$\nu = \frac{z}{h(t)}, \quad \text{and} \quad \tau = t \frac{|\dot{h}(0)|}{h(0)}. \tag{16}$$

The form of g is to be determined and this gives boundary conditions of the form

$$g(0, \tau) = 0, \quad g'(0, \tau) = 0, \tag{17}$$
$$g(1, \tau) = 1, \quad g'(1, \tau) = 0, \tag{18}$$

when the system is started from rest.

11

(3.5.4)   The Weissenberg number is defined to be $W_i = t_r \frac{|\dot{h}|}{h}$. Engmann *et al.* [5] considered solutions for large Weissenberg numbers (which are what we are probably dealing with in this case) and we find that in the limit $W_i \to \infty$ the leading order behaviour for g is

$$g_0 = 3\nu^2 - 2\nu^3, \tag{19}$$

that is the limit is the same as for the viscous case for a Newtonian Fluid. Phan-Thien and Walsh [9] contains a wide range of behaviour properties for materials undergoing squeeze film testing. If further data was available to determine parameter values for the explosives of interest, then this could be a very fruitful line of enquiry.

4   Numerical methodologies

4.1   LS-Dyna verses ABAQUS

(4.1.1)   In the initial presentation of the problem [4], numerical simulations were shown for the Steven test on an explosive with an elasto-plastic constitutive relation using the commercial code LS-Dyna. The results presented show heating near the upper and lower surfaces of the explosive which are inferred to be the result of frictional effects and the dissipation of energy. For large deformations the simulations break down because:

- there are skewed cells in the mesh, which cause the meshing to collapse;
- the fracture of the covering plate is not included.

(4.1.2)   The study group considered alternative methods for the simulation of the Steven test using ABAQUS, an alternative commercial solver. This alternative code allows large deformations to occur by exploiting adaptive mesh refinement and can capture the cracking of the top plate. Simulations of the Steven test using ABAQUS are available in the literature [6].

(4.1.3)   The study group attempted to replicate the simulation of the Steven test using ABAQUS. The correct rheology, incorporating an appropriate yield criteria for the explosive was not considered. However, the results produced demonstrate the effectiveness and ability of this solver for dealing with large deformations and the fracture of the covering plate. Figures 9 and 10 show stresses induced in the covering plate as the impactor hits, deforms and finally breaks through to the other side.
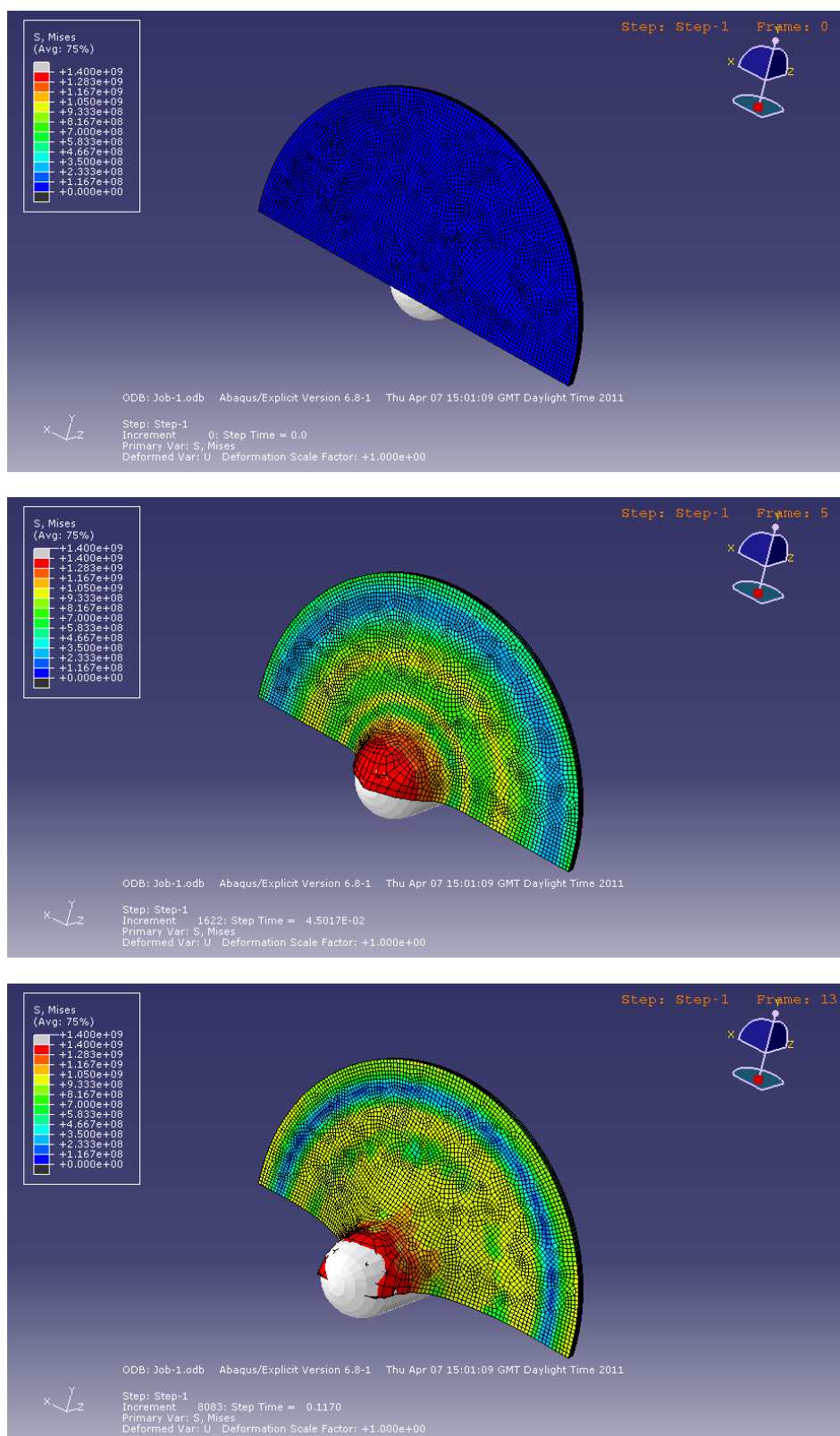
Figure 9: Three time snapshots showing a three-dimensional projectile *(i)* hitting the cover plate, *(ii)* deforming the cover plate out of the way and *(iii)* finally breaking through the cover plate into the region containing explosive.
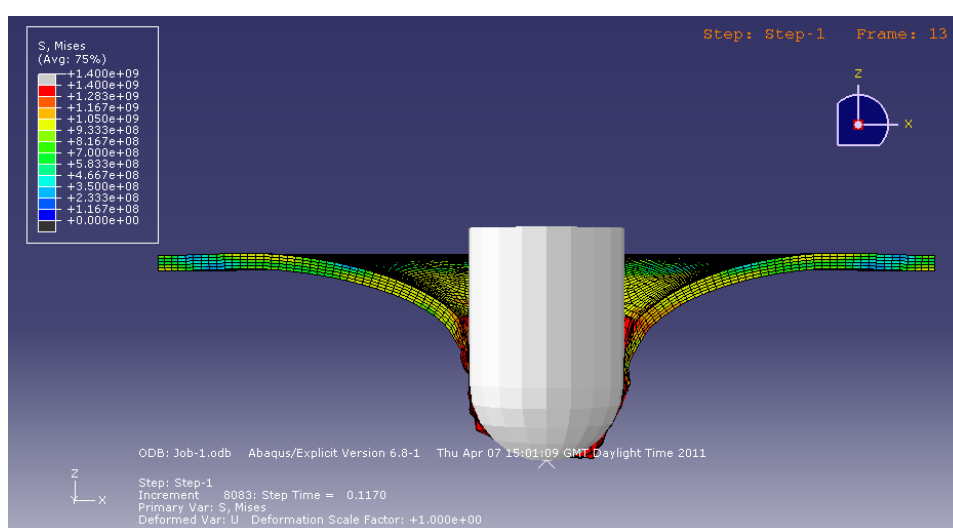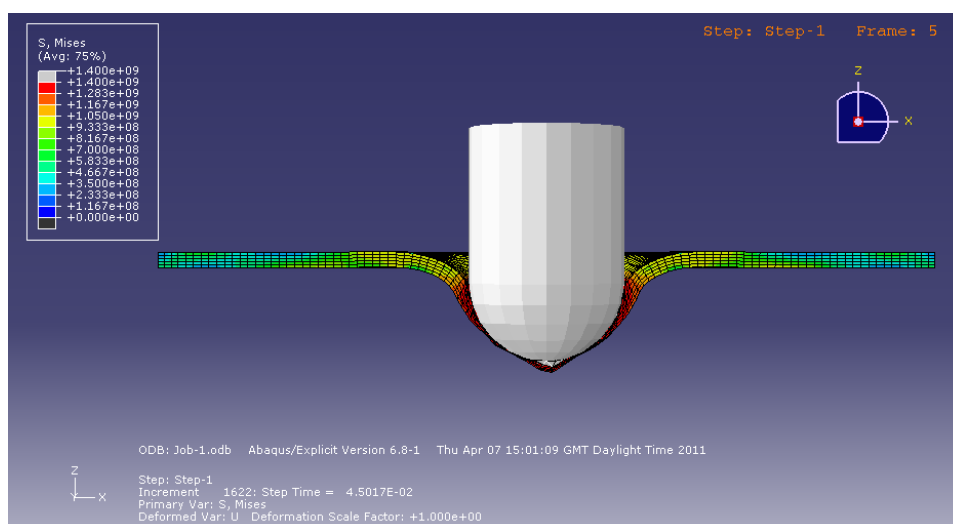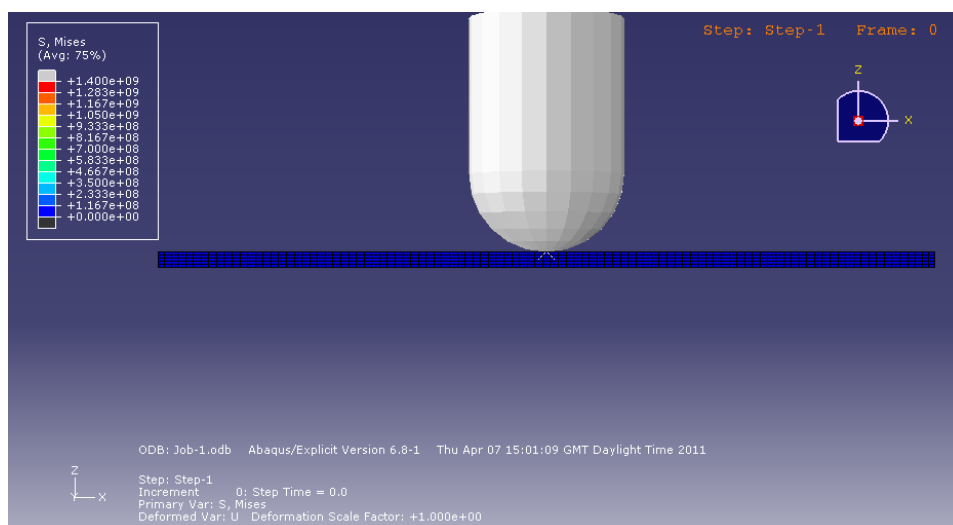
13

Figure 10: As figure 9, but viewed in the xz-plane.

5 Conclusions

5.1 Other potential experiments

(5.1.1)   The work undertaken by the study group highlighted several deficiencies in the current understanding of the material behaviour of explosives. Many different rheologies to model explosives under compression were discussed. However, the study group feels that further experimentation would be valuable to accurately determine the constitutive relationship of the explosive samples tested and their response to compression. The study group suggests that the results of the following experiments would be valuable and that AWE might like to investigate their practicality:

- Pinch Test: Compression of a sample between two parallel plates without confinement in the radial direction (see figure 6). The removal of the confining ring as seen in the Steven test and the flat top plate simplifies the geometry making it easier to analyse the results and compare with analytical models.
- Simple shearing: With an explosive sample fastened between two parallel plates, the top plate is moved parallel to the lower plate maintaining a constant gap width (see Figure 5). This motion induces a pure shear within the explosive sample and is potentially the easiest geometry to analyse.
- Cone Rheometry: Another standard rheological test that might be useful is cone rheometry. A cone rheometer can be used to analyse the behaviour of a thin layer of a viscoelastic material under conditions that are close to pure shear. It would be interesting to see whether the strain softening behaviour observed in the unconfined compression tests are replicated under shearing, and whether evidence of shear banding can be obtained.

(5.1.2)   The study group appreciates that some experiments that one might like to attempt are impossible due to the dangerous nature of explosives. Cutting a sample of explosive after an insult to look for shear banding is an example of a possible experiment that cannot be conducted with live explosives for safety reasons. However, the study group notes that in the past, inert surrogate explosives have been used to safely conduct compression tests. Replacing the explosives components within a polymer bonding with granulated sugar with a range of grain sizes has previously been shown to produce material samples with properties similar to explosives [8].

5.2 Summary

(5.2.1) The experimental evidence of tests on granular explosives held together by polymer bonding agents and the broader experience of the study group participants in the field of plasticity, both suggest that shear banding is the likely primary mechanism for plasticity in explosive samples subjected to compression. In this case plastic flow is localised about the shear bands, where there is a corresponding localised energy release. In the vicinity of the shear bands the temperature will be raised, potentially triggering ignition.

(5.2.2) AWE are interested in explosives with a wide range of potential rheologies; for both the creation of new explosive materials and to provide analytical test cases against which numerical codes can be validated. The study group investigated several different potential rheologies. In cases where the velocity of the sample is reduced where it comes into contact with the solid boundaries, the greatest dissipation of energy occurs close to the boundary and heat is generated in these areas, which is consistent with numerical simulations produced by AWE.

(5.2.3) The current numerical investigations of the Steven test conducted by AWE make use of the commerical code LS-Dyna. The study group identified that the meshes generated by this comerical code struggled to capture the large mesh deformations associated with high compression. Another commerical code ABAQUS was identified as a potential alternative. ABAQUS uses adaptive mesh refinement to improve highly deformed meshes and was also shown capable of modelling the rupture and breakup of the covering plate in the Steven test.

Bibliography

[1] J. E. Balzer, J. E. Field, M. J. Gifford, W. G. Proud, and S. M. Walley. High-speed photographic study of the drop-weight impact response of ultrafine and conventional PETN and RDX. *Combustion and Flame*, 130(4):298–306, 2002.

[2] J. W. Bebernes and A. A. Lacey. Shear band formation for a non-local model of thermo-viscoelastic flows. *Advances in Mathematical Sciences and Applications*, 15:265–282, 2005.

[3] S. P. Clancy, J. N. Johnson, and M. W. Burkett. Modeling the viscoelastic and brittle fracture response of high explosive in an Eulerian hydrocode. In *11th International Detonation Symposiam, 30 Aug – 4 Sep, Snowmass, CO, USA.*, 1998.

[4] J. Curtis. Modelling of the effects of friction and compression on explosives. In *Introductory presentation. ESGI 80 Cardiff*, 2011.

[5] J. Engmann, C. Servais, and A. S. Burbidge. Squeeze flow theory and applications to rheometry: A review. *Journal of Non-Newtonian Fluid Mechanics*, 132(1-3):1–27, 2005.

[6] C. Gruau, D. Picart, R. Belmas, E. Bouton, F. Delmaire-Sizes, J. Sabatier, and H. Trumel. Ignition of a confined high explosive under low velocity impact. *International Journal of Impact Engineering*, 36(4):537–550, 2009.

[7] P. D. Howell. *Mathematical Modeling: Case Studies from Industry*, chapter 1 - Fluid-Mechanical Modelling of the Scroll Compressor, pages 22–45. Cambridge, 2001.

[8] D. J. Idar, P. D. Peterson, P. D. Scott, and D. J. Funk. Low strain rate compression measurements of pbxn-9, pbx 9501, and mock 9501. *AIP Conference Proceedings*, 429(1):587–590, 1998.

[9] N. Phan-Thien and W. Walsh. Squeeze-film flow of an oldroyd-b fluid: Similarity solution and limiting weissenberg number. *Zeitschrift für Angewandte Mathematik und Physik (ZAMP)*, 35(6):747–759, 1984.

[10] J. D. Sherwood and D. Durban. Squeeze flow of a power-law viscoplastic solid. *Journal of Non-Newtonian Fluid Mechanics*, 62(1):35–54, 1996.

[11] C.-Y. Wang. The squeezing of a fluid between two plates. *Journal of Applied Mechanics*, 43(4):579–583, 1976.

[12] D. M. Williamson, C. R. Siviour, W. G. Proud, S. J. P. Palmer, R. Govier, K. Ellis, P. Blackwell, and C. Leppard. Temperature-time response of a polymer bonded explosive in compression (EDC37). *Journal of Physics D: Applied Physics*, 41(8):085404, 2008.

[13] T. W. Wright. *The Physics and Mathematics of Adiabatic Shear Bands*. Cambridge University Press, 2002.

[14] T. W. Wright and H. Ockendon. A scaling law for the effect of inertia on the formation of adiabatic shear bands. *International Journal of Plasticity*, 12(7):927–934, 1996.

[15] T. W. Wright and J. W. Walter. On stress collapse in adiabatic shear bands. *Journal of the Mechanics and Physics of Solids*, 35(6):701–720, 1987.